



An inverse dielectric mixing model at 50MHz that considers soil organic carbon

Chang-Hwan Park¹, Aaron Berg², Michael H. Cosh³, Andreas Colliander⁴, Andreas Behrendt⁵, Hida Manns², Jinkyu Hong⁶, Johan Lee¹ and Volker Wulfmeyer⁵

- 5 ¹National Institute of Meteorological Sciences, Earth System Research Division, Korea Meteorological Administration
²Department of Geography, Environment and Geomatics, University of Guelph, Guelph, ON N1G 2W1, Canada
³United States Department of Agriculture, Agricultural Research Service, Hydrology and Remote Sensing Laboratory, Beltsville, MD 20705, USA
⁴Jet Propulsion Laboratory, California Institute of Technology, Pasadena, CA 91109, USA
10 ⁵Institute of Physics and Meteorology, University of Hohenheim, Stuttgart 70599, Germany
⁶Ecosystem-Atmosphere Process Lab., Dep. of Atmospheric Science, Yonsei Univ., Seoul, 03722 Republic of Korea

Correspondence to: Chang-Hwan Park (ecomm77@gmail.com or chpark2@kma.go.kr)

Abstract. The prevalent soil moisture probe algorithms are based on a polynomial function that does not account for the variability in soil organic matter. Users are expected to choose a model before application: either a model for mineral soil or a model for organic soil. Both approaches inevitably suffer from limitations with respect to estimating the volumetric soil water content in soils having a wide range of organic matter content. In this study, we propose a new algorithm based on the idea that the amount of soil organic matter (SOM) is related to major uncertainties in the in-situ soil moisture data obtained using soil probe instruments. To test this theory, we derived a multiphase inversion algorithm from a physically based dielectric mixing model capable of using the SOM amount, performed a selection process from the multiphase model outcomes, and tested whether this new approach improves the accuracy of soil moisture (SM) data probes. The validation of the proposed new soil probe algorithm was performed using both gravimetric and dielectric data from the Soil Moisture Active Passive Validation Experiment in 2012 (SMAPVEX12). The new algorithm is more accurate than the previous soil-probe algorithm, resulting in a slightly improved correlation (0.824 \rightarrow 0.848), 12 % lower root mean square error (RMSE; 0.0824 \rightarrow 0.0725 cm³·cm⁻³), and 90 % less bias (-0.0042 \rightarrow 0.0004 cm³·cm⁻³). These results suggest that applying the new dielectric mixing model together with global SOM estimates will result in more reliable soil moisture reference data for weather and climate models and satellite validation.

1. Introduction

Soil moisture (SM) plays a critical role in weather and climate by affecting atmospheric variables via latent and sensible heat exchange. For example, near-surface air temperature can be affected by the evapotranspiration of surface and root zone soil moisture. Therefore, its correlation with the near-surface temperature is usually considered an effective indicator of the coupling strength between the land surface and the atmosphere (Seneviratne et al., 2006; Koster et al., 2009; Seneviratne et



al., 2010; Jaeger and Seneviratne, 2011; Seneviratne et al., 2013; Hirschi et al., 2014, p.; Whan et al., 2015). In particular, soil moisture anomalies in a dry regime have been reported as the main cause of strong land-atmosphere coupling, which can trigger drought and heat waves (Fischer et al., 2007; Zampieri et al., 2009; Hirschi et al., 2011; Miralles et al., 2011; Mueller and Seneviratne, 2012; Taylor et al., 2012; Guillod et al., 2015; Hauser et al., 2016; Seo et al., 2019). Soil moisture also influences precipitation formation and storm tracks by coupling with the atmosphere (Koster et al., 2004; Taylor et al., 2012; Guillod et al., 2015; Santanello et al., 2018, 2019; Zhang et al., 2019). Consequently, inaccurate SM information in the land-surface-model hinders accurate predictions of extreme climate and weather because of unrealistic land-atmosphere interactions that result from uncertainties in air temperature, moisture, dynamics, cloud formation, and precipitation.

High-quality in situ soil moisture data are an important reference for evaluating climate models (Yuan and Quiring, 2017; Zhuo et al., 2019) and remote-sensed SM data (Entekhabi et al., 2010; Kerr et al., 2010). However, it is not practically possible to perform in situ SM measurements with high spatial and temporal coverage. A practical alternative is to employ a portable soil probe that is calibrated using locally measured soil moisture. In particular, portable dielectric sensors make use of the relationship between the dielectric constant and volumetric soil water content. However, such retrieval of the volumetric soil water content from dielectric measurements does not account for soil organic matter (SOM) and saturation conditions. A few studies have reported the relationship between the dielectric constant and the volumetric soil water content in organic-rich soils (Topp et al., 1980; Roth et al., 1992; Bircher et al., 2012). However, the calibration functions derived from these studies have limitations for global-scale applications because they were developed using only a few specific sites and/or applicable only for the sites with a limited range of organic matter content. For the purpose of a global soil moisture probe observing system, using an inversion method of the existing physical dielectric mixing model can be a great alternative approach to incorporate the variability of organic matter into the probe algorithm beyond the current empirical probe models.

With this background, this work provides a pathway for a physical model to consider soil organic matter. We developed an inverse dielectric mixing model for mineral soil derived from (Park et al., 2017, 2019) to obtain more accurate volumetric soil moisture estimates from the dielectric constant. The proposed model reflects the damping effect and simulates the supersaturation of soil moisture over soil porosity (when soil moisture occupied larger than porosity of dry compacted soil in the unit volume causing light weight clay swelling or starting existence of standing water or starting surface runoff due to the precipitation accumulation over soil surface faster than infiltration) so that we can capture the standing water and surface runoff during flood events, which has not been studied in other prevalent dielectric mixing models

The most recent high resolution SOM map (Hengl et al., 2014; Batjes, 2016) is only available as a static variable for the land model; therefore, the realism of the parameterization for surface runoff, infiltration, evapotranspiration, and soil respiration is limited. Therefore, the other aim of this study is to provide a foundation for global SOM estimation using observations from a satellite, such as Soil Moisture Active Passive (SMAP), by developing a dielectric mixing model based on accurate in-situ SOM and gravimetric soil moisture.

The remainder of this paper is organized as follows: Section 2 introduces the inversion approach of dielectric mixing model to estimate soil moisture from organic soil using the probe. The data used in this study are described in Sect. 3. In Sect. 4, we



evaluate the results using the soil moisture measured during SMAPVEX12. Finally, a summary and discussion for further applications are provided in Sect. 5.

2. Method

Dielectric constant indicates a polarizability of materials at certain wavelength. The dipole structure of water molecule is highly sensitive to microwave electric field having very high dielectric constant approximately 80. On the other hand, the dielectric constant of soil mineral at microwave is rarely reacting having only low value from 3 to 5. Therefore, an instrument which can measure the effective dielectric constant of soil medium such as Stevens Hydraprobe can provide the accurate information of water amount within soil (Jackson et al., 1982; Schmugge, 1983; Stafford, 1988). Also, from the space, microwave satellite such as SMAP (Soil Moisture Active Passive) (Entekhabi et al., 2010), SMOS (Soil Moisture and Ocean Salinity) (Wigneron et al., 2007) and AMSR-E (Advanced Microwave Scanning Radiometer for EOS) can effectively estimate soil moisture from the measured brightness temperature by relating the effective dielectric constant of land surface.

For the application of portable soil probe, the in situ soil moisture data are provided based on the empirical relationship between the measured dielectric constant and the volumetric soil moisture (Seyfried and Murdock, 2004; Bell et al., 2013) using the following equation:

$$w = 0.0838\sqrt{\varepsilon_{\text{obs}}} - 0.0846 \quad (1)$$

where, ε_{obs} is the real part of the dielectric constant measured with the soil probe, and w is the estimation of the volumetric soil moisture ($\text{cm}^3 \cdot \text{cm}^{-3}$). As apparent in Eq. (1), the dependence of ε_{obs} on SOM was not considered in the estimation of w .

To consider the SOM, we first derive Eqs. (2)–(4), based on Park et al. (2019).

If the observed real part of the dielectric constant measured with the soil probe is smaller than the real part of the dielectric constant at the wilting point, $\varepsilon_{\text{obs}} < \varepsilon_{\text{wp}}$, we obtain:

for $w < w_{\text{wp}}$

$$w = a((\varepsilon_{\text{obs}} - 1)H^{-1} + 1) + b \quad (2)$$

where,

$$a = 1/\varepsilon_{\text{bound}}$$

$$b = -\frac{(1-p)\varepsilon_{\text{soil}} + p\varepsilon_{\text{air}}}{\varepsilon_{\text{bound}}}$$

where, H is the damping factor (0.8), $\varepsilon_{\text{bound}}$, is the dielectric constant for bound water, $\varepsilon_{\text{free}}$, dielectric constant for free water, ε_{air} is the dielectric constant for air (1).

95



If the observed real part of the dielectric constant measured with the soil probe is larger than the real part of the dielectric constant at the wilting point and still smaller than the saturation point, $\epsilon_{wp} < \epsilon_{obs} < \epsilon_p$, we get:

for $w_{wp} < w < p$

$$w = a\sqrt{(\epsilon_{obs} - 1)H^{-1} + c} + b \quad (3)$$

100 where,

$$a = \sqrt{(p - w_{wp}) / (\epsilon_{free} - \epsilon_{bound})}$$

$$b = \frac{w_{wp}\epsilon_{free} - p\epsilon_{bound}}{\sqrt{(p - w_{wp})(\epsilon_{free} - \epsilon_{bound})}}$$

$$c = \frac{(w_{wp}\epsilon_{free} - p\epsilon_{bound})^2}{4(p - w_{wp})(\epsilon_{free} - \epsilon_{bound})} - \epsilon_{soil} + \epsilon_{air}$$

105 Finally, for $\epsilon_{obs} > \epsilon_p$, we get:

for $p < w$

$$w = a((\epsilon_{obs} - 1)H^{-1} + 1) + b \quad (4)$$

$$a = \frac{1}{\epsilon_{free} - \epsilon_{soil}}$$

$$b = -\frac{\epsilon_{soil}}{\epsilon_{free} - \epsilon_{soil}}$$

110

For frequencies from 1.4 GHz to 50 MHz, the clay content is empirically considered in the dielectric constant for free, bound water, and dried organic soil at 50 MHz, as shown in Eq. (5–7).

$$\epsilon_{free} = \epsilon_{free1.4GHz} + 65 \cdot v_{clay} \quad (5)$$

$$\epsilon_{bound} = \epsilon_{bound1.4GHz} + 5 \cdot v_{clay} \quad (6)$$

$$115 \quad \epsilon_{soil} = (\epsilon_{clay} \cdot v_{clay} + \epsilon_{sand} \cdot v_{sand} + \epsilon_{silt} \cdot v_{silt})(1 - v_{SOM}) + \epsilon_{SOM} \cdot v_{SOM} \quad (7)$$

where, $\epsilon_{free\ 1.4GHz}$ and $\epsilon_{bound\ 1.4GHz}$ are the dielectric constant for free and bound water at 1.4GHz, respectively and v_{clay} , v_{silt} and v_{sand} are the volumetric ratios ($\text{cm}^3 \cdot \text{cm}^{-3}$) for clay, silt and sand, respectively.

The volumetric ratio of organic matter (v_{SOM} , $\text{cm}^3 \cdot \text{cm}^{-3}$) can be estimated from the organic matter and the bulk density (BD_{SOM}) using the following equation:

$$120 \quad v_{SOM} = \left(\left(\frac{1}{SOM} - 1 \right) \left(\frac{BD_{soil}}{BD_{SOM}} \right) + 1 \right)^{-1} \quad (8)$$



In this study, BD_{soil} was 1.2301 g cm^{-3} and the BD_{SOM} used in Eq. (8) is computed using the following non-linear model (Périer and Ouimet, 2011).

$$125 \quad BD_{SOM} = -1.977 + 4.105 \cdot \text{SOM} - 1.229 \cdot \ln(\text{SOM}) - 0.103 \cdot (\ln(\text{SOM}))^2 \quad (9)$$

where SOM is the mass of organic matter per mass of soil (kg SOM kg^{-1} soil).

In a previous study, Eq. (11) was proposed as the wilting point, which is a function of SOM ($\text{kg} \cdot \text{kg}^{-1}$) (Park et al., 2019). In
 130 our study, and the porosity is suggested as a power law function according to the SOM variable, as shown in Eq. (12).

$$w_{wp} = 0.02982 + 0.089 \cdot v_{clay} + 0.786 \cdot \text{SOM} \quad (11)$$

$$p = 0.18 + 0.26 \cdot v_{clay} + 0.54 \cdot \text{SOM}^{0.5} \quad (12)$$

By applying Eqs. (11) and (12), which require Eq. (8), Eqs. (2–4) can be used to compose the inverse dielectric mixing model
 135 for organic soil (IDO). A detailed description of the parameters used in the algorithm is provided in Table 1.

Table 1. Required physical properties to inverse the dielectric mixing model

Symbol	Physical property	Physical unit
ϵ_{obs}	Dielectric constant (real part) measured by TDR instrument	-
ϵ_{bound}	Dielectric constant (real part) of bound water at 50MHz	-
ϵ_{free}	Dielectric constant (real part) of free water at 50MHz	-
$\epsilon_{bound \ 1.4GHz}$	Dielectric constant (real part) of bound water at 1.4GHz	-
$\epsilon_{free \ 1.4GHz}$	Dielectric constant (real part) of free water at 1.4GHz	-
ϵ_{soil}	Dielectric constant (real part) of dry soil	-
ϵ_{air}	Dielectric constant (real part) of air	-
p	Dry porosity or saturation point	$\text{cm}^3 \cdot \text{cm}^{-3}$
w_{wp}	Wilting point [$\text{cm}^3 \text{cm}^{-3}$]	$\text{cm}^3 \cdot \text{cm}^{-3}$
H	Damping factor [-]	-
w	Volumetric soil water	$\text{cm}^3 \cdot \text{cm}^{-3}$
v_{clay}	Volumetric mixing ratio of clay	$\text{cm}^3 \cdot \text{cm}^{-3}$
v_{silt}	Volumetric mixing ratio of silt	$\text{cm}^3 \cdot \text{cm}^{-3}$
v_{sand}	Volumetric mixing ratio of sand	$\text{cm}^3 \cdot \text{cm}^{-3}$
v_{SOM}	Volumetric mixing ratio of soil organic matter	$\text{cm}^3 \cdot \text{cm}^{-3}$
OC	Organic carbon	$\text{g} \cdot \text{kg}^{-1}$



OM	Organic matter	%
BD	Bulk density	$\text{g}\cdot\text{cm}^{-3}$
PD	Solid particle density	$\text{kg}\cdot\text{m}^{-3}$

SOM is expressed as organic carbon (OC) in the majority of global soil maps (Hugelius et al., 2013; Hengl et al., 2014; Batjes, 2016; Hengl et al., 2017; “Harmonized world soil database v1.2 | FAO SOILS PORTAL,” 2020), as well as in the published units in the SMAPVEX 12 study (Manns and Berg, 2014). Organic carbon is the major component of SOM, and in order to convert OC to SOM, the conversion factor (f_{oc}) of 1.8 was used in Eq (10).

$$\text{SOM} = f_{oc} \cdot \text{OC} \quad (10)$$

The conventional OC-to-SOM conversion factor was proposed to be 1.724 by (Waksman and Stevens, 1930; Stenberg et al., 2010). However, it has been reported that the OC-to-SOM conversion factor can vary from 1.25 to 2.5, and the conventional value of 1.724 tends to overestimate the OC, as reported by Pribyl (2010). Instead of 1.724, 1.8 is a more appropriate value for a wide range of OC, as supported by various studies (Broadbent, 1953; Ranney, 1969; Manns and Berg, 2014). Therefore, in this study, we applied 1.8 for the conversion factor f_{oc} in Eq. (10).

The IDO model is composed of bound, mixed, and free water models, as shown in Fig. 1(a–c), respectively. The selection process for the model parameters is shown in Fig. 1(d) and requires the dielectric constant values to be estimated from the known wilting point and porosity, along with ϵ_{wp} and ϵ_p values to retrieve the soil moisture value from the measured dielectric constant. Instead of estimating them, we selected the second largest measured SM value. We found that in an S-like stepwise model, the second order in SM magnitude is the proper method to select Eqs. 2, 3, or 4 without the knowledge of ϵ_{wp} and ϵ_p . Additionally, selecting the lowest or highest value for a given measurement along the x-axis might be a valid selection process for any type of concave or convex-like stepwise model.

The difference in the soil moisture estimation from the observed dielectric constant based on the Seyfried and IDO models is presented in Fig. 1(e). The IDO model provides larger SM values with high SOM input (purple curve) and lower SM values in low SOM input (orange curve) compared to the Seyfried model (black dotted curve). The factory setting (default probe algorithm) reflects the average SOM effect empirically in the generalized model. Even with medium-range SOM (red curve), a relatively small but more complex difference between the two approaches can be revealed in the SM estimation: lower SM estimation in wet soil and higher SM estimation in dry soil than the probe estimated (black dotted).

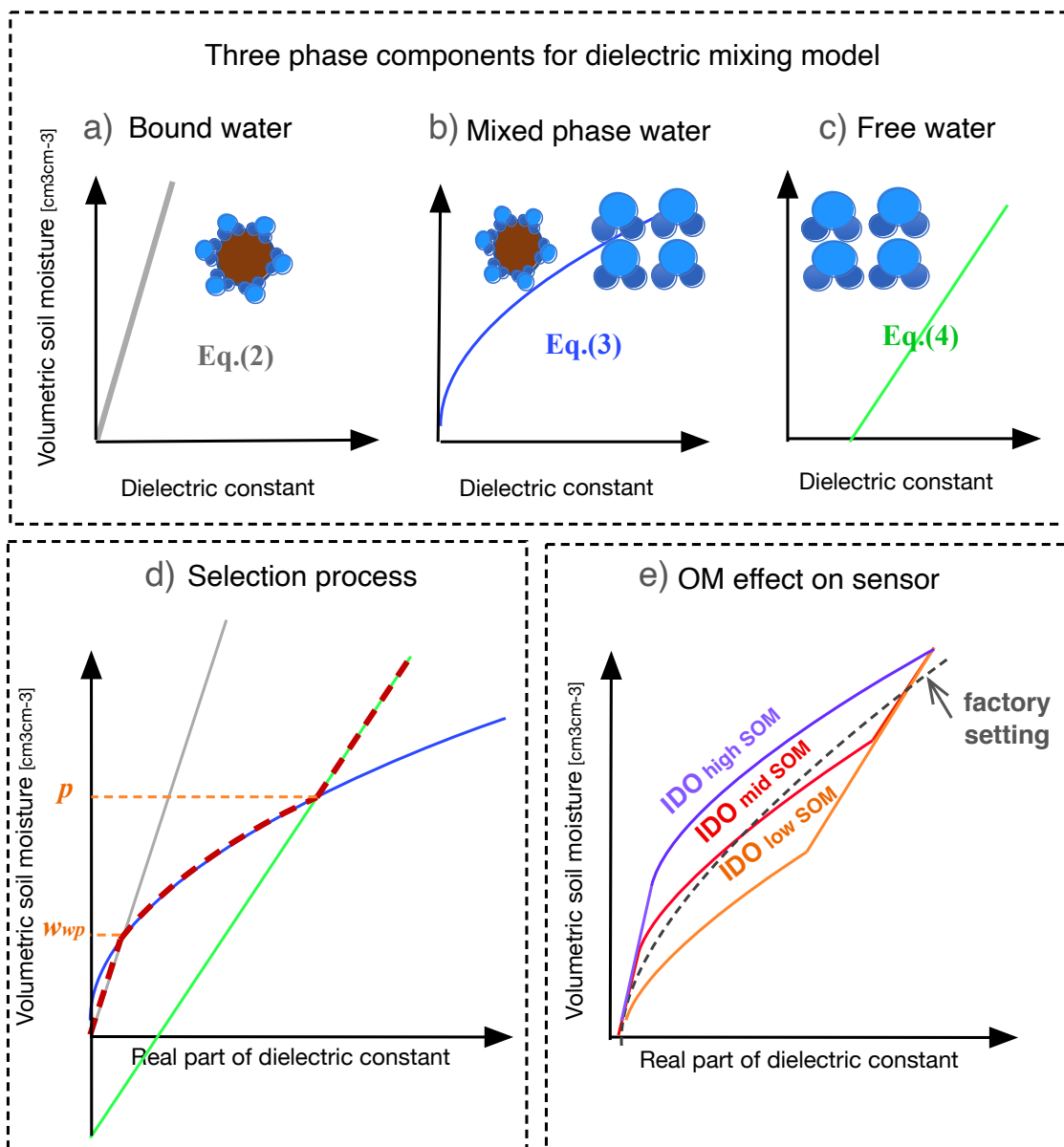


Figure 1: Single phase relationship between (a) dielectric constant and bound water, (b) bound and free water mixture, (c) free water, (d) selection process among those models, and (e) comparison with the polynomial-based soil probe sensor algorithm proposed by Seyfried (Seyfried and Murdock, 2004) and for organic soils (IDO)

3. Data

First, it was necessary to determine whether including the organic matter parameter in the dielectric mixing model improves the accuracy of soil moisture estimation from the probed dielectric constant. Thus, we compared the results with the SM measured using the gravimetric method during SMAPVEX12. The SMAPVEX12 field campaign took place in 2012 (southwest of Winnipeg, Manitoba, Canada), and the SMAP SM retrieval algorithms were calibrated and validated before the launch of the SMAP satellite in 2015 (McNairn et al., 2015). During this field campaign, intensive data of the L-band brightness temperature and back-scattering albedo were collected using airborne sensors. The land surface type, crop type, soil texture (clay and sand contents), the real part of the dielectric constant from soil moisture probes with the field average of 16 sampling data obtained in every second day from June 6 to July 17, 2013). The sampling depth of the probe is established as top 5cm soil which layer is relevant to the brightness temperature emission depth detectable by SMOS and SMAP (Schmugge, 1983; Jackson et al., 1997) and gravimetrically determined volumetric soil moisture at the ground sites were measured on the ground by sampling soils with 4.7 cm diameter x 4.6 cm depth (Mann and Berg, 2013). For comparison with our new model, we used probe measurements (real dielectric constant) as the input and volumetric soil moisture data as references (Rowlandson et al., 2013), which were simultaneously archived with microwave brightness temperature measured from airborne NASA's L-band active-passive PALS instrument. The ancillary information for this function (soil texture information) was provided by (Bullock et al., 2014). At the SMAPVEX12 validation sites (Fig. 2a), the volumetric clay and sand mixing ratios for Eqs. 5, 6, 7, 11, and 12 are from the Agriculture and Agri-Food Canada (AAFC) Soil Landscapes of Canada database (Government of Canada, n.d.). The OC information was sampled from the SoilGrid1km database (Hengl et al., 2014) and compared to the field estimates of the OC put forth by Manns and Berg (2014).

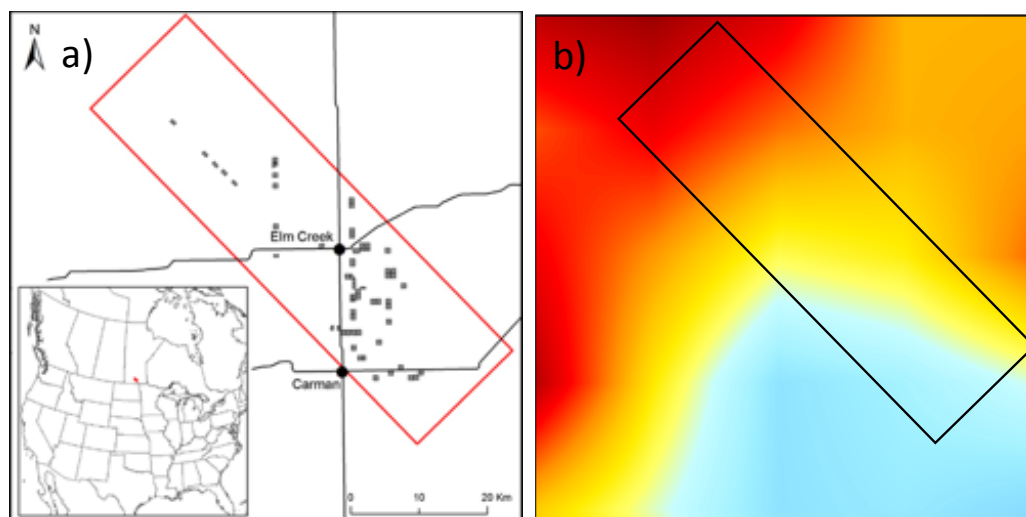


Figure 2: (a) SMAPVEX12 validation sites (adapted from (Rowlandson et al., 2013)) and (b) calculated distribution of soil organic matter in Canada based on the SoilGrid1km database.

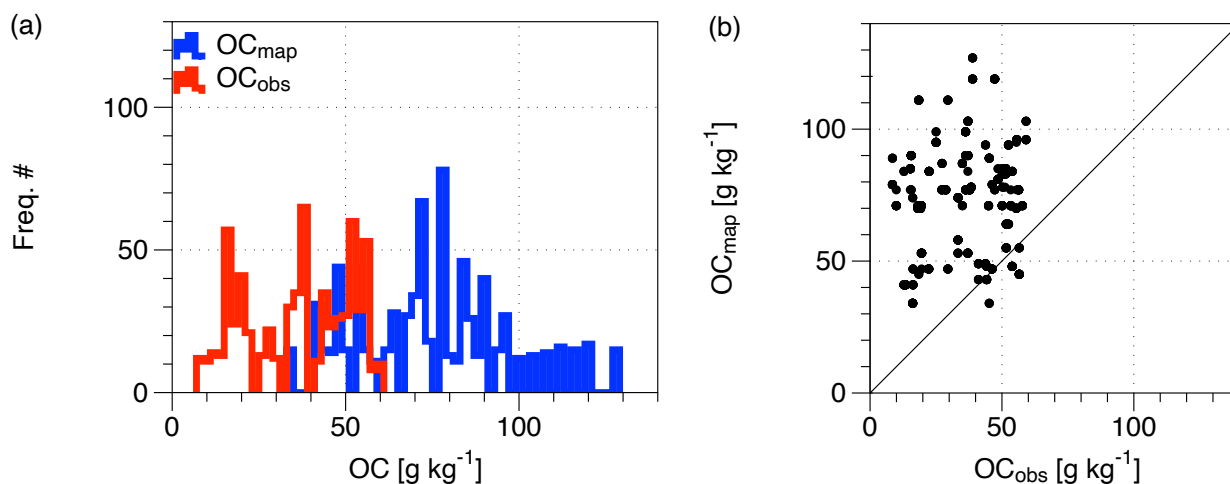


There are significant range differences among the global soil organic carbon maps (Zhu et al., 2019), such as the HWSD (“Harmonized world soil database v1.2 | FAO SOILS PORTAL,” 2020), SoilGrid1km (Hengl et al., 2014), WISE30sec (Batjes, 2016), and Northern Circumpolar Soil Carbon Database (NCSCD; Hugelius et al., 2013). Therefore, the reliability of the global soil organic maps used for local soil moisture estimation using soil probes is still unknown. To investigate the potential limitation of global OC maps (hereafter called the OC_{map} experiment), we performed a comparison of OC measurements obtained from each SMAPVEX12 site (Manns and Berg, 2014) with those retrieved from the SoilGrid1km map. As shown in Fig. 3(a), there is an offset between both datasets of $\sim 50 \text{ g}\cdot\text{kg}^{-1}$. The estimated OC from the map was greater and showed a wider OC range compared to the measured OC in the SMAPVEX12 sites (Fig. 3b). This means that the SoilGrid250m (Hengl et al., 2017) estimates are, on average, more than 100 % higher than the measured data. Thus, a potential limitation of the SoilGrid250m map exists not only in the spatial pattern, but also in the overall magnitude ($74.4 \text{ g}\cdot\text{kg}^{-1}$ in average). In this study, we used OC from SoilGrid250m (without any scaling factor) for the OC_{map} experiment.

195

200

We investigated the OC accuracy using one type of OC input into the new soil probe algorithm (Eqs. 2–4) by performing two experiments: 1) OC entered using a SoilGrid250m map (OC_{map} experiment; blue in Fig. 3) and 2) SMAPVEX12 the OC in situ of SMAPVEX12 (red in Fig. 3).



205

Figure 3: Comparison between organic carbon (OC) observation from SMAPVEX12 (red) and data sampled from highly resolved SoilGrid250m map (Hengl et al., 2017) (blue) in: (a) in histogram and (b) in scatter plot.

4. Calibration of portable soil-moisture sensors

The development of the calibration models is necessary for further campaigns or further extension of the global soil moisture network based on a portable soil moisture sensor. For example, calibration models (Rowlandson et al., 2013) were proposed by deriving the parameters A , B , and C of the quadratic function between the effective dielectric constant and soil moisture for each SMAPVEX12 station.

210



$$\varepsilon = Aw^2 + Bw + C \quad (13)$$

In each site a unique set of A , B and C was obtained to estimate w (volumetric soil moisture) from the measured dielectric constant ε . It is important to verify whether these empirical models are transferable to other field sites based on physical interpretation. Therefore, we compared them with those derived from the dielectric mixing model, as shown in Table 2. The weighting function describing the attenuation of signal on probe and satellite sensor can be an exponential form basically following Beer-Lamber law where infinite attenuation of the electric field is allowed but negligible for the deeper than sampling depth. On the other hand, a quadratic form can be considered as the weighting function based on the assumption of linearly decreasing refractive index scheme (Wilheit, 1978) so that the emission can be assumed to be zero from the deeper sampling depth. In this study, as shown in Table 2, we assumed the Beer-Lamber law to consider the attenuation effect by applying the damping factor 0.8 applicable both for probe and satellite remote sensing. More detail derivation associated with the damping factor can be found in the previous study (Park et al., 2017).

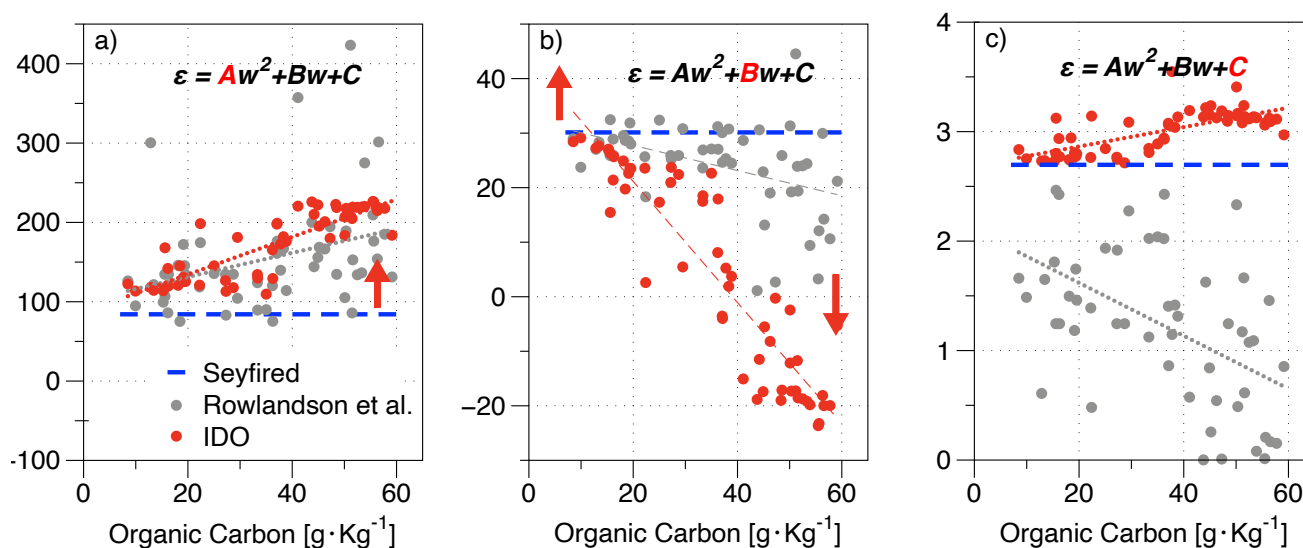
Table 2. A, B, and C parameters of the relationship between the effective dielectric constant and soil moisture adapted from (Park et al., 2017) with damping factor H (0.8) ; dielectric constant for free ($\varepsilon_{\text{free}}$), bound water ($\varepsilon_{\text{bound}}$) and soil mineral including organic matter ($\varepsilon_{\text{soil}}$).

w range	A	B	C
$w < w_{\text{wp}}$	0	$(\varepsilon_{\text{bound}} - 1) \cdot H$	$((1 - p)\varepsilon_{\text{soil}} + p) \cdot H + H - 1$
$w_{\text{wp}} < w < p$	$\frac{\varepsilon_{\text{free}} - \varepsilon_{\text{bound}}}{p - w_{\text{wp}}} \cdot H$	$\frac{p\varepsilon_{\text{bound}} - w_{\text{wp}}\varepsilon_{\text{free}}}{p - w_{\text{wp}}} \cdot H$	$(1 - p)\varepsilon_{\text{soil}} \cdot H + H - 1$
$p < w$	0	$(\varepsilon_{\text{free}} - \varepsilon_{\text{soil}}) \cdot H$	$\varepsilon_{\text{soil}} \cdot H + H - 1$

We observed that when the wilting point and porosity increased with increasing OC [according to Eqs. (11–12)], A and B increased and decreased, respectively, as shown in Fig. 4. The results of this matching (Fig. 4) showed that A and B used in the quadratic function computed for SMAPVEX12 can be parameterized with soil texture, wilting point, porosity, and the bound and free water dielectric constants. Additionally, the C parameter indicates the effective dielectric constant of the mixture of dry organic matter (approximately 1.2 (Savin et al., 2020)) and solid mineral soil (3-5); ideally, the C parameter value should decrease with an increase in OC. Notably, the clay content was also positively correlated with an increase in OC in the SMAPVEX12. Therefore, owing to the simultaneous increase in clay content, which is characterized by a high dielectric constant, the sensitivity of the C parameter to OC variation (decreasing pattern in C) is nullified, as shown in Fig. 4(c). Furthermore, because C perfectly represents the dielectric constant of dry soil, it should be greater than 1, which is the real part of the dielectric constant of a vacuum. Based on this physical constraint, the previous C (gray points in Fig. 4) is unrealistically low (less than that of the vacuum state) in the higher SOM range. The minimum C is $(1-p)\varepsilon_{\text{soil}}$ among three w



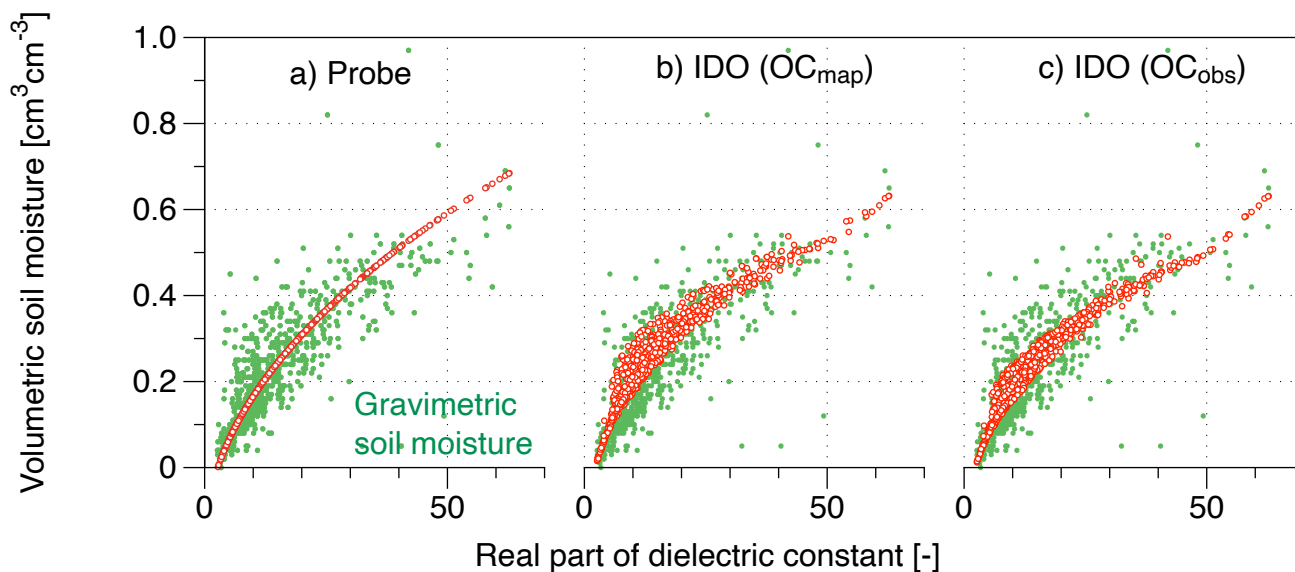
240 ranges [Eq. (4)] because the following order is always true $[(1-p)\epsilon_{\text{soil}} < (1-p)\epsilon_{\text{soil}} + p < \epsilon_{\text{soil}}]$ and it is larger than 2 as shown in Fig. 4 C. This shows that the proposed IDO computes a more realistic value of dielectric constant for organic soil.



245 **Figure 4: Relationship between soil organic carbon measurements (x-axis) and calibration parameters (A , B and C) (y-axis) relating between measured dielectric constant (ϵ) and volumetric soil moisture (w): (blue dash lines) A , B , C which are not sensitive to OC measurements (Seyfried approach); (gray dots) A , B , C which are empirically obtained (Rowlandson et al., 2013); (red dots) A , B , C which are physically simulated by proposed IDO which applies the wilting point and porosity as functions of sand and clay volumetric mixing ratios as well as soil organic carbon with the damping factor applied.**

250 5. Results

This study aimed to mitigate a significant discrepancy found between volumetric soil moisture estimated by soil probe sensor (considered as ground truth for the validation of land surface modeling and remote sensing) and the gravimetric soil moisture. Therefore, in this section, the new approach proposed in the section 2 was investigated whether the accuracy of the new sensor algorithm can be improved comparing to the existing probe algorithm. Firstly, looking at the Fig. 5(a) the current issue in the probe SM estimates was well displayed in terms of the matching pattern of the gravimetric soil moisture with the measured dielectric constant. It showed that the existing probe soil moisture (red dots in Fig.5(a)) couldn't follow both features appeared in the measurements (the significant scattering degree and the distinct varying patterns in dry and wet condition). This is a fundamental limitation of the traditional polynomial function, the Seyfried model as well as a two-mode system (mineral or organic soil), as proposed by Topp et al. (1980) or (Roth et al., 1992).



260

Figure 5: Scatter plot between probe measurements of the real part of the dielectric constant (x-axis) and volumetric soil moisture (y-axis) measured by gravimetric method (green dots in a, b, c), Seyfried model (black dots in a), IDO with SOM taken from SoilGrid250m (Hengl et al., 2017) (red dots in b) and IDO using OC measured during SMAPVEX12 (Manns and Berg, 2014) (red dots in c).

265

On the other hand, the IDO, soil organic carbon considered, allowed us to compute SM with similar scattering pattern comparable to the measured by gravimetric method. It means that soil organic carbon is critical factor for the application of the soil moisture sensor from portable to satellite based. In the regards of the shape appearing in the scattering pattern, IDO captured the distinctively curved edge in the low and high-end points close to the values of 12 and 50, respectively, in the x-axis for the real part of the dielectric constant. Only difference between b) and c) at Fig.5 is OC input, originated from SoilGrid250m or from in-situ obtained during SMAPVEX12, respectively, with the same input of clay and sand mixing ratio from SMAPVEX 12. This pattern is probably related to the transition moments from bound to mixed (a to b in Fig. 1) and from mixed to free water states (b to c in Fig.1), which is a very interesting evidence indicating that soil probes can detect critical soil parameters such as wilting point and soil porosity based on the accumulated dielectric measurements of certain sites.

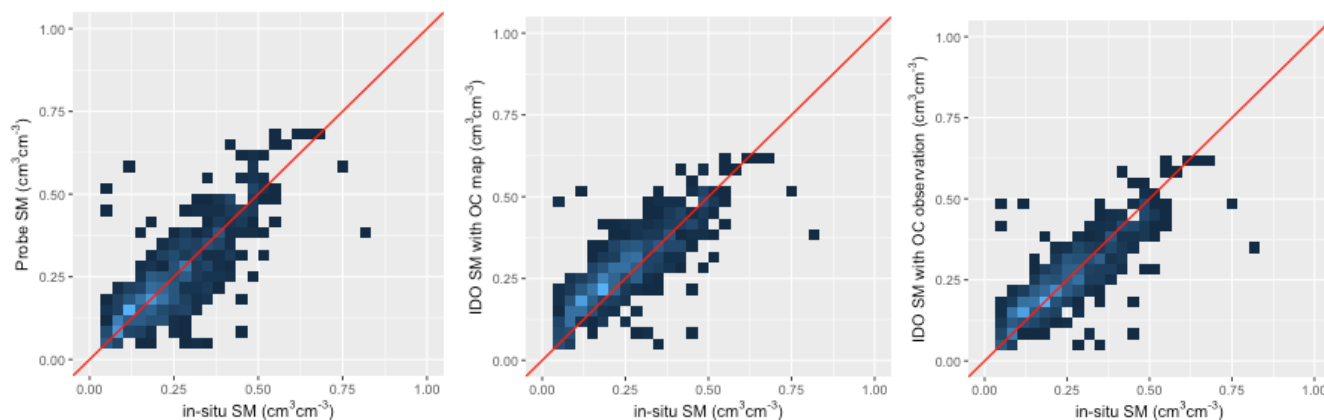
275

Even though, the shape of SM scattering estimated from the measured dielectric data (x-axis) became similar to the one appeared in the gravimetric soil moisture, it is also required to investigate about whether the actual improvement in the SM accuracy has been achieved via the point-by-point comparison with the gravimetric data. This analysis was illustrated in the Q-Q plot in Fig.6. It displayed that the scattered uncertainty shown in Fig. 6(a) of the current soil probe algorithm can be reduced by IDO approach as (b) and (c). The scatter error shown in Fig.6(a) slightly converged into a 1:1 line when the IDO adapted the OC map as input (b) and further improved with a narrower scattered error pattern with OC in situ (c). This result

280



further supported that the OC variability with the proposed model can mitigate the uncertainty in SM estimation of the current dielectric-based soil moisture sensor network.

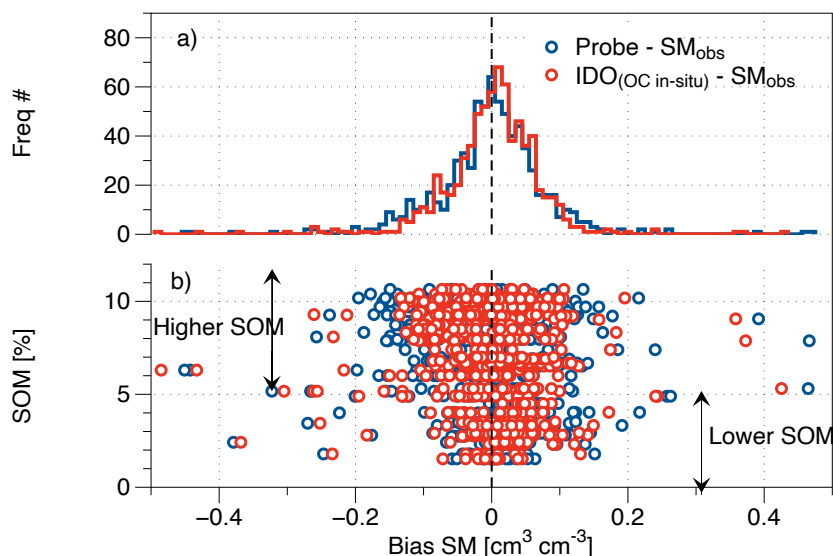


285 **Figure 6: Performance of soil moisture probe algorithms in terms of scattering degree to the gravimetric measurements (x-axis); soil moisture estimates (y-axis) using a) 3rd order polynomial approach (Bell et al., 2013; Seyfried and Murdock, 2004), b) the proposed inverse dielectric mixing model (IDO) with the variational soil organic matter (SOM) sampled from the SoilGrid1km map (Hengl et al., 2017) and c) the same algorithm but with SOM measured from SMAPVEX12 (Manns and Berg, 2014).**

290

In Fig. 7, we investigated more characteristics of SM uncertainty: how the biases of SM estimated by the conventional probe algorithm are related to the in situ OC and whether they can be mitigated by the proposed algorithm with the OC measurements. Fig. 7(a) shows that both negative and positive biases are affected by the IDO. Fig. 7(b), obtained by spreading out the histogram according to the degree of SOM, provides an in-depth analysis on how these biases are distributed according to the measured SOM. This shows that the negative bias in the high SOM range was reduced because the polynomial function of the conventional probe algorithm presented in Fig. 1(e) tends to overestimate the SM in the cases of lower SOM and underestimate the SM in cases of higher SOM (as compared to the proposed multiphase model).

295



300 **Figure 7: (a) Histogram of soil moisture (SM) bias and (b) its scatter relationship according to soil organic matter (SOM) converted from in-situ organic carbon (OC)**

The importance of accurate and highly resolved organic carbon data in soil moisture estimation from portable soil sensors is well evident from the statistical validation presented in Table 3. The results confirmed that the IDO performs better than the
 305 traditional probe algorithm based on a 3rd order polynomial function specially with the OC measured in the SMAPVEX12 field campaign (with a maintained spatial variability); RMSE = 0.0761 cm³·cm⁻³, correlation of 0.8476, and bias of -0.0014 cm³·cm⁻³.

310 **Table 3. Validation of soil moisture obtained from Probe (Probe SM), organic soil based on SoilGrid250m organic carbon map (IDO_{map}), and SMAPVEX12 OC in situ observation (IDO_{obs})**

	Bias	RMSE	Correlation
Probe	-0.0042	0.0824	0.824
Proposed algorithm with organic carbon map (IDO _{map})	0.0266	0.0807	0.833
Proposed algorithm with in situ organic carbon (IDO _{obs})	0.0004	0.0725	0.849

The results in this section demonstrated that the wilting point and porosity which emerged in paring the gravimetric soil moisture and the dielectric measurements, could be detected also by new model. Also, it is proved that the volumetric soil moisture could be estimated from the sensor more accurately in terms of bias, RMSE and correlation analysis. It means that
 315 our approach can provide more accurate soil moisture probe algorithm than currently used in various soil moisture network such as USCRN (US Surface Climate Observing Reference Networks) and the SMAPVEX field campaigns. In the boreal

forest and Alaska Tundra region with abundant SOM, our study can deliver a significant effect to the validation and conclusion of the previous studies in land surface modeling and microwave satellite remote sensing, which used the probe soil moisture as a reference data.

320 6. Summary and discussion

In this study, we proposed an inverse dielectric mixing model for a 50-MHz soil sensor for agricultural organic soil. This model is composed of three nonlinear functions that are mathematically capable of describing the physical behavior, including the effect of the organic matter content. It is also noticed that the used organic matter carbon data sampled from SMAPVEX12 sites ($36 \text{ g}\cdot\text{kg}^{-1}$) was half that of the OC map ($74 \text{ g}\cdot\text{kg}^{-1}$). The validation results demonstrated a higher performance of the new model. Regardless of the small amount of OC, its effect improved the performance of the SM estimation, which was demonstrated via the IDO proposed in this study. We compared the obtained soil-moisture retrievals with improved RMSE (13% ↓), slightly stronger correlation (3%↑), and lower bias (90%↓) using the new model and gravimetric soil moisture data. But still the coverage of the simulated pattern over the measured points was smaller. Therefore, we sought out a potential further improvement based on the additional experiment designed with OM varying within the proposed model. The simulation based on the conventional polynomial function (red curve in the Fig. 8 (a)) could not reduce the innate uncertainties and the IDO proposed in this study could resolve this issue. However, the red dots simulated with IDO (Fig. 8(b)) covered over the measured green dots insufficiently. Therefore, in order to activate this weak pattern we performed the experiments to impose a more dynamic OC estimate to investigate whether greater or less SOM can cover a similar boundary of the measured distribution through the IDO model. The results showed that the piecewise pattern of SM simulated with the proposed approach well covered the measured pattern with imposing lower (1 %) to higher (30 %) SOM.

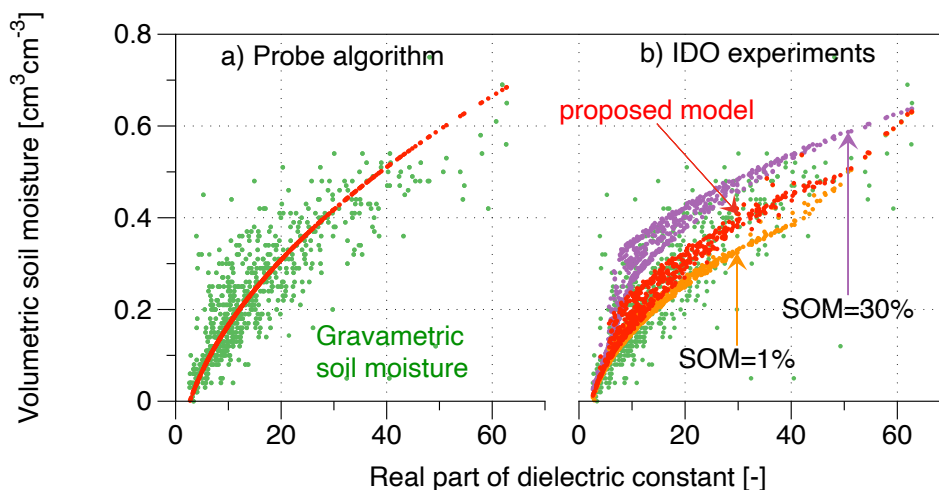




Figure 8: Investigation of the similarity of the scatter pattern between the measured dielectric constant and the soil moisture: (a) obtained from the gravimetric measurements and (b) experimentally simulated with extreme soil organic matter (SOM) from 0 % to 30 %.

340

Because the SOM is translated from OC with a conversion factor (1.8) in this study, the improvement might had been not sufficient. A realistic estimation of the conversion factor (f_{oc}) in Eq. (10) varying from 1.25 up to 2.5 might be a possible solution for this. In addition, the IDO is a model able to replace the calibration factors A , B , and C of Eq. (13) with the soil properties presented in Table.2. Overall, the proposed more physics based IDO can replace the current soil probe sensor algorithm, which does not incorporate the importance of organic matter variability.

345

A significant improvement could not be shown probably due to two reasons: the instrumental error in measuring OC from soil sample or the constant OC to SOM conversion factor (1.8 for all soil samples). In addition, uncertainty can be suspected from other sources, such as clay or sand contents or soil salinity (assumed to be 0 % in this study) used in the IDO. These effects on the dielectric measurements and their uncertainties probably served as the limitation of further improvement by the IDO.

350

Nevertheless, the results regarding the adaptation of in-situ OC in our study demonstrated that the accuracy of the OM input for IDO is critical for the accuracy of SM estimation from the probe sensor. Furthermore, we anticipate that the proposed approach will be more effective in obtaining a more realistic SM from soil probe sensors in organic soils.

355

360

365

370



Author contributions:

CHP developed the algorithm. CHP, AB, MHC, AC and HM designed the study. HM collected the soil organic carbon in-situ data. CHP conducted the validation and the analysis. JH, AB, JL and VW provided guidance on the research direction. CHP wrote the manuscript. All authors reviewed the manuscript.

375 Acknowledgement:

This work was funded by the Korea Meteorological Administration Research and Development Program “Development of Climate Prediction System” under Grant (KMA2018-00322). The USDA is an equal opportunity employer and provider. A partial contribution to this work was made at the Jet Propulsion Laboratory, California Institute of Technology under a contract with National Aeronautics and Space Administration and a National Research Foundation of Korea Grant from the Korean
380 Government (MSIT) (NRF-2018R1A5A1024958).

Funding:

Declaration of Interest: The authors declare that they have no conflict of interest.

385 References

- Batjes, N.H., 2016. Harmonized soil property values for broad-scale modelling (WISE30sec) with estimates of global soil carbon stocks. *Geoderma* 269, 61–68. <https://doi.org/10.1016/j.geoderma.2016.01.034>
- Bell, J.E., Palecki, M.A., Baker, C.B., Collins, W.G., Lawrimore, J.H., Leeper, R.D., Hall, M.E., Kochendorfer, J., Meyers, T.P., Wilson, T., Diamond, H.J., 2013. U.S. Climate Reference Network Soil Moisture and Temperature Observations. *J. Hydrometeorol.* 14, 977–988. <https://doi.org/10.1175/JHM-D-12-0146.1>
- 390 Birchak, J.R., Gardner, C.G., Hipp, J.E., Victor, J.M., 1974. High dielectric constant microwave probes for sensing soil moisture. *Proc. IEEE* 62, 93–98. <https://doi.org/10.1109/PROC.1974.9388>
- Bircher, S., Skou, N., Jensen, K.H., Walker, J.P., Rasmussen, L., 2012. A soil moisture and temperature network for SMOS validation in Western Denmark. *Hydrol. Earth Syst. Sci.* 16, 1445–1463. <https://doi.org/10.5194/hess-16-1445-2012>
- 395 Broadbent, F.E., 1953. The Soil Organic Fraction, in: Norman, A.G. (Ed.), *Advances in Agronomy*. Academic Press, pp. 153–183. [https://doi.org/10.1016/S0065-2113\(08\)60229-1](https://doi.org/10.1016/S0065-2113(08)60229-1)
- Bullock, Paul, Berg, Aaron, Wiseman, Grant, 2014. SMAPVEX12 Core-Based Soil Texture Data, Version 1. <https://doi.org/10.5067/376D19WSS9VT>
- Dobson, M.C., Ulaby, F.T., Hallikainen, M.T., El-rayes, M.A., 1985. Microwave Dielectric Behavior of Wet Soil-Part II: Dielectric Mixing Models. *IEEE Trans. Geosci. Remote Sens.* GE-23, 35–46. <https://doi.org/10.1109/TGRS.1985.289498>
- 400 Fischer, E.M., Seneviratne, S.I., Vidale, P.L., Lüthi, D., Schär, C., 2007. Soil Moisture–Atmosphere Interactions during the 2003 European Summer Heat Wave. *J. Clim.* 20, 5081–5099. <https://doi.org/10.1175/JCLI4288.1>



- Government of Canada, A. and A.-F.C., n.d. Canadian Soil Information Service [WWW Document]. URL <https://sis.agr.gc.ca/cansis/> (accessed 3.3.21).
- 405 Guillod, B.P., Orlowsky, B., Miralles, D.G., Teuling, A.J., Seneviratne, S.I., 2015. Reconciling spatial and temporal soil moisture effects on afternoon rainfall. *Nat. Commun.* 6, 6443. <https://doi.org/10.1038/ncomms7443>
- Hallikainen, M.T., Ulaby, F.T., Dobson, M.C., El-rayes, M.A., Wu, L., 1985. Microwave Dielectric Behavior of Wet Soil-Part 1: Empirical Models and Experimental Observations. *IEEE Trans. Geosci. Remote Sens.* GE-23, 25–34. <https://doi.org/10.1109/TGRS.1985.289497>
- 410 Harmonized world soil database v1.2 | FAO SOILS PORTAL, 2020.
- Hauser, M., Orth, R., Seneviratne, S.I., 2016. Role of soil moisture versus recent climate change for the 2010 heat wave in western Russia. *Geophys. Res. Lett.* 43, 2819–2826. <https://doi.org/10.1002/2016GL068036>
- Hengl, T., Jesus, J.M. de, Heuvelink, G.B.M., Gonzalez, M.R., Kilibarda, M., Blagotić, A., Shangguan, W., Wright, M.N., Geng, X., Bauer-Marschallinger, B., Guevara, M.A., Vargas, R., MacMillan, R.A., Batjes, N.H., Leenaars, J.G.B., Ribeiro, E.,
- 415 Wheeler, I., Mantel, S., Kempen, B., 2017. SoilGrids250m: Global gridded soil information based on machine learning. *PLOS ONE* 12, e0169748. <https://doi.org/10.1371/journal.pone.0169748>
- Hengl, T., Jesus, J.M. de, MacMillan, R.A., Batjes, N.H., Heuvelink, G.B.M., Ribeiro, E., Samuel-Rosa, A., Kempen, B., Leenaars, J.G.B., Walsh, M.G., Gonzalez, M.R., 2014. SoilGrids1km — Global Soil Information Based on Automated Mapping. *PLOS ONE* 9, e105992. <https://doi.org/10.1371/journal.pone.0105992>
- 420 Hirschi, M., Mueller, B., Dorigo, W., Seneviratne, S.I., 2014. Using remotely sensed soil moisture for land–atmosphere coupling diagnostics: The role of surface vs. root-zone soil moisture variability. *Remote Sens. Environ.* 154, 246–252. <https://doi.org/10.1016/j.rse.2014.08.030>
- Hirschi, M., Seneviratne, S.I., Alexandrov, V., Boberg, F., Boroneant, C., Christensen, O.B., Formayer, H., Orlowsky, B., Stepanek, P., 2011. Observational evidence for soil-moisture impact on hot extremes in southeastern Europe. *Nat. Geosci.* 4,
- 425 17–21. <https://doi.org/10.1038/ngeo1032>
- Hugelius, G., Bockheim, J.G., Camill, P., Elberling, B., Grosse, G., Harden, J.W., Johnson, K., Jorgenson, T., Koven, C.D., Kuhry, P., Michaelson, G., Mishra, U., Palmtag, J., Ping, C.-L., O’Donnell, J., Schirrmeyer, L., Schuur, E. a. G., Sheng, Y., Smith, L.C., Strauss, J., Yu, Z., 2013. A new data set for estimating organic carbon storage to 3 m depth in soils of the northern circumpolar permafrost region. *Earth Syst. Sci. Data* 5, 393–402. <https://doi.org/10.5194/essd-5-393-2013>
- 430 Jaeger, E.B., Seneviratne, S.I., 2011. Impact of soil moisture–atmosphere coupling on European climate extremes and trends in a regional climate model. *Clim. Dyn.* 36, 1919–1939. <https://doi.org/10.1007/s00382-010-0780-8>
- Kerr, Y.H., Waldteufel, P., Wigneron, J.-P., Delwart, S., Cabot, F., Boutin, J., Escorihuela, M.-J., Font, J., Reul, N., Gruhier, C., Juglea, S.E., Drinkwater, M.R., Hahne, A., Martin-Neira, M., Mecklenburg, S., 2010. The SMOS Mission: New Tool for Monitoring Key Elements of the Global Water Cycle. *Proc. IEEE* 98, 666–687. <https://doi.org/10.1109/JPROC.2010.2043032>
- 435 Koster, R.D., Dirmeyer, P.A., Guo, Z., Bonan, G., Chan, E., Cox, P., Gordon, C.T., Kanae, S., Kowalczyk, E., Lawrence, D., Liu, P., Lu, C.-H., Malyshev, S., McAvaney, B., Mitchell, K., Mocko, D., Oki, T., Oleson, K., Pitman, A., Sud, Y.C., Taylor,



- C.M., Verseghy, D., Vasic, R., Xue, Y., Yamada, T., 2004. Regions of Strong Coupling Between Soil Moisture and Precipitation. *Science* 305, 1138–1140. <https://doi.org/10.1126/science.1100217>
- 440 Koster, R.D., Schubert, S.D., Suarez, M.J., 2009. Analyzing the Concurrence of Meteorological Droughts and Warm Periods, with Implications for the Determination of Evaporative Regime. *J. Clim.* 22, 3331–3341. <https://doi.org/10.1175/2008JCLI2718.1>
- Manns, H.R., Berg, A.A., 2014. Importance of soil organic carbon on surface soil water content variability among agricultural fields. *J. Hydrol., Determination of soil moisture: Measurements and theoretical approaches* 516, 297–303. <https://doi.org/10.1016/j.jhydrol.2013.11.018>
- 445 McNairn, H., Jackson, T.J., Wiseman, G., Belair, S., Berg, A., Bullock, P., Colliander, A., Cosh, M.H., Kim, S.-B., Magagi, R., Moghaddam, M., Njoku, E.G., Adams, J.R., Homayouni, S., Ojo, E., Rowlandson, T., Shang, J., Goita, K., Hosseini, M., 2015. The Soil Moisture Active Passive Validation Experiment 2012 (SMAPVEX12): Prelaunch Calibration and Validation of the SMAP Soil Moisture Algorithms. *IEEE Trans. Geosci. Remote Sens.* 5, 2784–2801. <https://doi.org/10.1109/TGRS.2014.2364913>
- 450 Miralles, D.G., Holmes, T.R.H., De Jeu, R. a. M., Gash, J.H., Meesters, A.G.C.A., Dolman, A.J., 2011. Global land-surface evaporation estimated from satellite-based observations. *Hydrol. Earth Syst. Sci.* 15, 453–469. <https://doi.org/10.5194/hess-15-453-2011>
- Mironov, V.L., Kosolapova, L.G., Fomin, S.V., 2009. Physically and Mineralogically Based Spectroscopic Dielectric Model for Moist Soils. *IEEE Trans. Geosci. Remote Sens.* 47, 2059–2070. <https://doi.org/10.1109/TGRS.2008.2011631>
- 455 Mueller, B., Seneviratne, S.I., 2012. Hot days induced by precipitation deficits at the global scale. *Proc. Natl. Acad. Sci.* 109, 12398–12403. <https://doi.org/10.1073/pnas.1204330109>
- Park, C.-H., Behrendt, A., LeDrew, E., Wulfmeyer, V., 2017. New Approach for Calculating the Effective Dielectric Constant of the Moist Soil for Microwaves. *Remote Sens.* 9, 732. <https://doi.org/10.3390/rs9070732>
- Park, C.-H., Montzka, C., Jagdhuber, T., Jonard, F., De Lannoy, G., Hong, J., Jackson, T.J., Wulfmeyer, V., 2019. A Dielectric
460 Mixing Model Accounting for Soil Organic Matter. *Vadose Zone J.* 18. <https://doi.org/10.2136/vzj2019.04.0036>
- Périé, C., Ouimet, R., 2011. Organic carbon, organic matter, and bulk density relationships in boreal forest soils. *Can. J. Soil Sci.* <https://doi.org/10.4141/CJSS06008>
- Pribyl, D.W., 2010. A critical review of the conventional SOC to SOM conversion factor. *Geoderma* 156, 75–83. <https://doi.org/10.1016/j.geoderma.2010.02.003>
- 465 Ranney, R.W., 1969. An Organic Carbon-Organic Matter Conversion Equation for Pennsylvania Surface Soils. *Soil Sci. Soc. Am. J.* 33, 809–811. <https://doi.org/10.2136/sssaj1969.03615995003300050049x>
- Roth, C.H., Malicki, M.A., Plagge, R., 1992. Empirical evaluation of the relationship between soil dielectric constant and volumetric water content as the basis for calibrating soil moisture measurements by TDR. *J. Soil Sci.* 43, 1–13. <https://doi.org/10.1111/j.1365-2389.1992.tb00115.x>



- 470 Rowlandson, T.L., Berg, A.A., Bullock, P.R., Ojo, E.R., McNairn, H., Wiseman, G., Cosh, M.H., 2013. Evaluation of several calibration procedures for a portable soil moisture sensor. *J. Hydrol.* 498, 335–344. <https://doi.org/10.1016/j.jhydrol.2013.05.021>
- Santanello, J.A., Dirmeyer, P.A., Ferguson, C.R., Findell, K.L., Tawfik, A.B., Berg, A., Ek, M., Gentine, P., Guillod, B.P., Heerwaarden, C. van, Roundy, J., Wulfmeyer, V., 2018. Land–Atmosphere Interactions: The LoCo Perspective. *Bull. Am. Meteorol. Soc.* 99, 1253–1272. <https://doi.org/10.1175/BAMS-D-17-0001.1>
- 475 Santanello, Jr.J.A., Lawston, P., Kumar, S., Dennis, E., 2019. Understanding the Impacts of Soil Moisture Initial Conditions on NWP in the Context of Land–Atmosphere Coupling. *J. Hydrometeorol.* 20, 793–819. <https://doi.org/10.1175/JHM-D-18-0186.1>
- Savin, I., Mironov, V., Muzalevskiy, K., Fomin, S., Karavayskiy, A., Ruzicka, Z., Lukin, Y., 2020. Dielectric database of organic Arctic soils (DDOAS). *Earth Syst. Sci. Data* 12, 3481–3487. <https://doi.org/10.5194/essd-12-3481-2020>
- 480 Seneviratne, S.I., Corti, T., Davin, E.L., Hirschi, M., Jaeger, E.B., Lehner, I., Orlowsky, B., Teuling, A.J., 2010. Investigating soil moisture–climate interactions in a changing climate: A review. *Earth-Sci. Rev.* 99, 125–161. <https://doi.org/10.1016/j.earscirev.2010.02.004>
- Seneviratne, S.I., Lüthi, D., Litschi, M., Schär, C., 2006. Land–atmosphere coupling and climate change in Europe. *Nature* 443, 205–209. <https://doi.org/10.1038/nature05095>
- 485 Seneviratne, S.I., Wilhelm, M., Stanelle, T., Hurk, B. van den, Hagemann, S., Berg, A., Cheruy, F., Higgins, M.E., Meier, A., Brovkin, V., Claussen, M., Ducharne, A., Dufresne, J.-L., Findell, K.L., Ghattas, J., Lawrence, D.M., Malyshev, S., Rummukainen, M., Smith, B., 2013. Impact of soil moisture–climate feedbacks on CMIP5 projections: First results from the GLACE-CMIP5 experiment. *Geophys. Res. Lett.* 40, 5212–5217. <https://doi.org/10.1002/grl.50956>
- 490 Seo, E., Lee, M.-I., Jeong, J.-H., Koster, R.D., Schubert, S.D., Kim, H.-M., Kim, D., Kang, H.-S., Kim, H.-K., MacLachlan, C., Scaife, A.A., 2019. Impact of soil moisture initialization on boreal summer subseasonal forecasts: mid-latitude surface air temperature and heat wave events. *Clim. Dyn.* 52, 1695–1709. <https://doi.org/10.1007/s00382-018-4221-4>
- Seyfried, M.S., Murdock, M.D., 2004. Measurement of Soil Water Content with a 50-MHz Soil Dielectric Sensor. *Soil Sci. Soc. Am. J.* 68, 394–403. <https://doi.org/10.2136/sssaj2004.3940>
- 495 Stenberg, B., Viscarra Rossel, R.A., Mouazen, A.M., Wetterlind, J., 2010. Chapter Five - Visible and Near Infrared Spectroscopy in Soil Science, in: Sparks, D.L. (Ed.), *Advances in Agronomy*. Academic Press, pp. 163–215. [https://doi.org/10.1016/S0065-2113\(10\)07005-7](https://doi.org/10.1016/S0065-2113(10)07005-7)
- Taylor, C.M., de Jeu, R.A.M., Guichard, F., Harris, P.P., Dorigo, W.A., 2012. Afternoon rain more likely over drier soils. *Nature* 489, 423–426. <https://doi.org/10.1038/nature11377>
- 500 Topp, G.C., Davis, J.L., Annan, A.P., 1980. Electromagnetic determination of soil water content: Measurements in coaxial transmission lines. *Water Resour. Res.* 16, 574–582. <https://doi.org/10.1029/WR016i003p00574>
- Waksman, S.A., Stevens, K.R., 1930. A CRITICAL STUDY OF THE METHODS FOR DETERMINING THE NATURE AND ABUNDANCE OF SOIL ORGANIC MATTER. *Soil Sci.* 30, 97–116.



- 505 Wang, J.R., Schmugge, T.J., 1980. An Empirical Model for the Complex Dielectric Permittivity of Soils as a Function of
Water Content. *IEEE Trans. Geosci. Remote Sens.* GE-18, 288–295. <https://doi.org/10.1109/TGRS.1980.350304>
- Whan, K., Zscheischler, J., Orth, R., Shongwe, M., Rahimi, M., Asare, E.O., Seneviratne, S.I., 2015. Impact of soil moisture
on extreme maximum temperatures in Europe. *Weather Clim. Extrem.*, The World Climate Research Program Grand
Challenge on Extremes – WCRP-ICTP Summer School on Attribution and Prediction of Extreme Events 9, 57–67.
<https://doi.org/10.1016/j.wace.2015.05.001>
- 510 Yuan, S., Quiring, S.M., 2017. Evaluation of soil moisture in CMIP5 simulations over the contiguous United States using in
situ and satellite observations. *Hydrol. Earth Syst. Sci.* 21, 2203–2218. <https://doi.org/10.5194/hess-21-2203-2017>
- Zampieri, M., D’Andrea, F., Vautard, R., Ciais, P., Noblet-Ducoudré, N. de, Yiou, P., 2009. Hot European Summers and the
Role of Soil Moisture in the Propagation of Mediterranean Drought. *J. Clim.* 22, 4747–4758.
<https://doi.org/10.1175/2009JCLI2568.1>
- 515 Zhang, F., Pu, Z., Wang, C., 2019. Impacts of Soil Moisture on the Numerical Simulation of a Post-Landfall Storm. *J. Meteorol.*
Res. 33, 206–218. <https://doi.org/10.1007/s13351-019-8002-8>
- Zhu, D., Ciais, P., Krinner, G., Maignan, F., Jornet Puig, A., Hugelius, G., 2019. Controls of soil organic matter on soil thermal
dynamics in the northern high latitudes. *Nat. Commun.* 10, 3172. <https://doi.org/10.1038/s41467-019-11103-1>